LEARNING TO DECEIVE KNOWLEDGE GRAPH AUGMENTED MODELS VIA TARGETED PERTURBATION

Anonymous authors
Paper under double-blind review

ABSTRACT

Knowledge graphs (KGs) have helped neural-symbolic models improve performance on various knowledge-intensive tasks, like question answering and item recommendation. By using attention over the KG, such models can also "explain" which KG information was most relevant for making a given prediction. In this paper, we question whether these models are really behaving as we expect. We demonstrate that, through a reinforcement learning policy (or even simple heuristics), one can produce deceptively perturbed KGs which maintain the downstream performance of the original KG while significantly deviating from the original semantics and structure. Our findings raise doubts about KG-augmented models' ability to leverage KG information and provide plausible explanations.

1 INTRODUCTION

Recently, neural reasoning over symbolic knowledge graphs (KGs) has emerged as a popular paradigm in machine learning. Such neural-symbolic KG (NSKG) models have improved performance on a number of knowledge-intensive downstream tasks: for question answering (QA), the KG provides context about how a given answer choice is related to the question (Lin et al., 2019; Feng et al., 2020; Lv et al., 2020; Talmor et al., 2018); for item recommendation (Wang et al., 2018b; 2019a;b; 2018a), the KG mitigates data sparsity and cold start issues. Furthermore, by using attention over the KG, such models can "explain" which KG information was most relevant for making a given prediction (Lin et al., 2019; Feng et al., 2020; Wang et al., 2018b; 2019b; Cao et al., 2019; Gao et al., 2019). Nonetheless, the process in which NSKG models reason about KG information is still not well understood. It is generally assumed that, like humans, NSKG models base their predictions on semantically meaningful chains of entities and relations in the KG and that this process is responsible for KG-associated performance gains (Lin et al., 2019; Feng et al., 2020; Gao et al., 2019; Song et al., 2019).

In this paper, we challenge the above assumption and question whether existing NSKG models actually use KGs in a faithful manner. We study this question primarily by measuring model performance when all edges in the KG have been perturbed. To perturb the KG, we propose four perturbation heuristics and a reinforcement learning (RL) based perturbation algorithm. Surprisingly, for NSKG models on both commonsense QA and item recommendation, we find that the KG can be extensively perturbed with little to no effect on performance. This raises doubts about the plausibility of KG-based explanations and the role of KGs in current NSKG models. To the best of our knowledge, we are the first to analyze the effects of targeted KG perturbations on NSKG model performance.

2 PROBLEM SETTING

Our goal is to investigate: **(A)** whether NSKG models faithfully use KGs for making predictions and **(B)** whether KGs facilitate plausible explanations of model predictions. For **(A)**, across different perturbation methods, we measure model performance when every edge in the KG has been perturbed. To quantify the extent to which the KG has been perturbed, we also measure both semantic and structural similarity between original KG and perturbed KG. Assuming the original KG contains accurate information, if original-perturbed KG similarity is low, then a faithful NSKG model should achieve worse performance with the perturbed KG than with the original KG. For **(B)**, we ask human subjects to rate original and perturbed KGs with respect to readability and usefulness for solving downstream tasks. If a KG receives higher ratings, then we can say that it is more likely to provide plausible explanations.

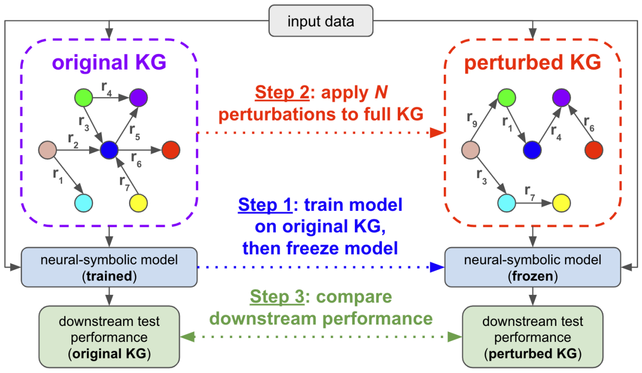
input data
original KG
perturbed KG
Step 2: apply N perturbations to full KG
Step 1: train model on original KG, then freeze model
neural-symbolic model (trained)
neural-symbolic model (frozen)
Step 3: compare downstream performance
downstream test performance (original KG)
downstream test performance (perturbed KG)

Figure 1: **Proposed KG Perturbation Framework.** Our procedure consists of three main steps: **(1)** train the NSKG model on the original KG, then freeze the model; **(2)** obtain the perturbed KG by applying $N = |\mathcal{T}|$ perturbations to the full original KG; and **(3)** compare the perturbed KG's downstream performance to that of the original KG.

Notation Let $\mathcal{F}_\theta$ be an NSKG model, and let $(X_{\text{train}}, X_{\text{dev}}, X_{\text{test}})$ be a dataset for some downstream task. We denote a KG as $\mathcal{G} = (\mathcal{E}, \mathcal{R}, \mathcal{T})$, where $\mathcal{E}$ is the set of entities (nodes), $\mathcal{R}$ is the set of relation types, and $\mathcal{T} = \{(e_1, r, e_2) \mid e_1, e_2 \in \mathcal{E},\ r \in \mathcal{R}\}$ is the set of facts (edges) composed from existing entities and relations. Let $\mathcal{G}' = (\mathcal{E}, \mathcal{R}', \mathcal{T}')$ be the KG obtained after perturbing $\mathcal{G}$, where $\mathcal{R}' \subseteq \mathcal{R}$ and $\mathcal{T}' \neq \mathcal{T}$. Let $f(\mathcal{G}, \mathcal{G}')$ be a function that measures similarity between $\mathcal{G}$ and $\mathcal{G}'$. Let $g(\mathcal{G})$ be the downstream performance when evaluating $\mathcal{F}_\theta$ on X_{test} and $\mathcal{G}$. Also, let $\oplus$ denote the concatenation operation, and let $\mathcal{N}_L(e)$ denote the set of L-hop neighbors for entity $e \in \mathcal{E}$.

High-Level Procedure First, we train $\mathcal{F}_\theta$ on X_{train} and $\mathcal{G}$, then evaluate $\mathcal{F}_\theta$ on X_{test} and $\mathcal{G}$ to get the original performance $g(\mathcal{G})$. Second, we freeze $\mathcal{F}_\theta$, then perturb $\mathcal{G}$ to obtain $\mathcal{G}'$. Third, we evaluate $\mathcal{F}_\theta$ on X_{test} and $\mathcal{G}'$ to get the perturbed performance $g(\mathcal{G}')$. Finally, we measure $g(\mathcal{G}) - g(\mathcal{G}')$ and $f(\mathcal{G}, \mathcal{G}')$ to assess how faithful the model is. This procedure is illustrated in Figure 1. In this paper, we consider two downstream tasks: commonsense QA and item recommendation.

Commonsense QA Given a question x and a set of k possible answers $\mathcal{A} = \{y_1, ..., y_k\}$, the task is to predict a compatibility score for each (x, y) pair, such that the highest score is predicted for the correct answer. In commonsense QA, the questions are designed to require commonsense knowledge which is typically unstated in natural language, but more likely to be found in KGs (Talmor et al., 2018). Let $\mathcal{F}_\phi^{\text{text}}$ be a Transformer text encoder, $\mathcal{F}_\psi^{\text{graph}}$ be a graph encoder, and $\mathcal{F}_\xi^{\text{cls}}$ be an MLP classifier, where $\phi, \psi, \xi \subset \theta$. Let $\mathcal{G}_{(x,y)}$ denote a subgraph of $\mathcal{G}$ consisting of entities mentioned in text sequence $x \oplus y$, plus their corresponding edges. We start by computing a text embedding $\mathbf{h}_{\text{text}} = \mathcal{F}_\phi^{\text{text}}(x \oplus y)$ and a graph embedding $\mathbf{h}_{\text{graph}} = \mathcal{F}_\phi^{\text{graph}}(\mathcal{G}_{(x,y)})$. After that, we compute the score for (x, y) as $S_{(x,y)} = \mathcal{F}_\xi^{\text{cls}}(\mathbf{h}_{\text{text}} \oplus \mathbf{h}_{\text{graph}})$. Finally, we select the highest scoring answer: $y_{\text{pred}} = \arg\max_{y \in A}\ S_{(x,y)}$. KG-augmented commonsense QA models vary primarily in their design of $\mathcal{F}_\psi^{\text{graph}}$. In particular, path-based models compute the graph embedding by using attention to selectively aggregate paths in the subgraph. The attention scores can help explain which paths the model focused on most for a given prediction (Lin et al., 2019; Feng et al., 2020; Santoro et al., 2017).

Item Recommendation We consider a set of users $\mathcal{U} = \{u_1, u_2, ..., u_m\}$, a set of items $\mathcal{V} = \{v_1, v_2, ..., v_n\}$, and a user-item interaction matrix $\mathbf{Y} \in \mathbb{R}^{m \times n}$. If user u has been observed to engage with item v, then $y_{uv} = 1$ in the user-item interaction matrix; otherwise, $y_{uv} = 0$. Additionally, we consider a KG $\mathcal{G}$, in which $\mathcal{R}$ is the set of relation types in $\mathcal{G}$. In $\mathcal{G}$, nodes are items $v \in \mathcal{V}$, and edges are facts of the form (v, r, v'), where $r \in \mathcal{R}$ is a relation. For the zero entries in $\mathbf{Y}$ (i.e., $y_{uv} = 0$), our task is to predict a compatibility score for user-item pair (u, v), indicating how likely user u is to want to engage with item v. We represent each user u, item v, and relation r as embeddings $\mathbf{u}$, $\mathbf{v}$, and $\mathbf{r}$, respectively. Given a user-item pair (u, v), its compatibility score is computed as $\langle \mathbf{u}, \mathbf{v} \rangle$, the inner product between $\mathbf{u}$ and $\mathbf{v}$. KG-augmented recommender systems differ mainly in how they use $\mathcal{G}$ to compute $\mathbf{u}$ and $\mathbf{v}$. Generally, these models do so by using attention to selectively aggregate items/relations in $\mathcal{G}$. The attention scores can help explain which items/relations the model found most relevant for a given prediction (Wang et al., 2018b; 2019b).

3 KG Similarity Metrics

To measure how much the perturbed KG has deviated from the original KG, we propose several metrics for capturing semantic (ATS) and structural (SC2D, SD2) similarity between KGs.

Aggregated Triple Score (ATS) ATS measures semantic similarity between two KGs. Let $s_\mathcal{G}$ be an edge (triple) scoring function, such that $s_\mathcal{G}(e_1, r, e_2)$ measures how likely edge (e_1, r, e_2) is to exist in $\mathcal{G}$. Also, assume $s_\mathcal{G}$ has been pre-trained on $\mathcal{G}$ for link prediction. Then, ATS is defined as $f_{\text{ATS}}(\mathcal{G}, \mathcal{G}') = \frac{1}{|\mathcal{T}'|} \sum_{(e_1,r,e_2) \in \mathcal{T}'} s_\mathcal{G}(e_1, r, e_2)$, which denotes the mean $s_\mathcal{G}$ score across all edges in $\mathcal{G}'$. Intuitively, if a high percentage of edges in $\mathcal{G}'$ are also likely to exist in $\mathcal{G}$ (i.e., high ATS), then we can say that $\mathcal{G}'$ and $\mathcal{G}$ have high semantic similarity. Note that the choice of $s_{\mathcal{G}}$ is task-specific, as KGs from different tasks may differ greatly with respect to semantics or structure. For commonsense QA, we use the $s_{\mathcal{G}}$ from Li et al. (2016); for item recommendation, we use the $s_{\mathcal{G}}$ from Yang et al. (2015). While ATS captures semantic KG differences, it is not sensitive to KG connectivity structure.

Similarity in Clustering Coefficient Distribution (SC2D) SC2D measures structural similarity between two KGs and is derived from the local clustering coefficient (Saramäki et al., 2007; Onnela et al., 2005; Fagiolo, 2007). For a given entity in $\mathcal{G}$ (treated here as undirected), the local clustering coefficient is the fraction of possible triangles through the entity that exist (i.e., how tightly the entity's neighbors cluster around it). For entity $e_i \in \mathcal{E}$, the local clustering coefficient is defined as $c_i = 2\text{Tri}(e_i)/(\deg(e_i)(\deg(e_i) - 1))$, where $\text{Tri}(e_i)$ is the number of triangles through e_i, and $\deg(e_i)$ is the degree of e_i. For each relation $r \in \mathcal{R}$, let $\mathcal{G}^r$ be the subgraph of $\mathcal{G}$ consisting of all edges in $\mathcal{T}$ with r . That is, $\mathcal{G}^r = (\mathcal{E}, r, \mathcal{T}^{'})$, where $\mathcal{T}^{'} = \{(e, r, e') \mid e, e' \in \mathcal{E}\}$. Let $\mathbf{c}^r$ denote the $|\mathcal{E}|$-dimensional clustering coefficient vector for $\mathcal{G}^r$, where the ith element of $\mathbf{c}^r$ is c_i. Then, the mean clustering coefficient vectors for $\mathcal{G}$ and $\mathcal{G}'$ are $\mathbf{c}_o = \frac{1}{|\mathcal{R}|}\sum_{r\in\mathcal{R}} \mathbf{c}^r$ and $\mathbf{c}_p = \frac{1}{|\mathcal{R}'|}\sum_{r\in\mathcal{R}'} \mathbf{c}^r$, respectively. Finally, SC2D is defined as $f_{\text{SC2D}}(\mathcal{G}, \mathcal{G}^{'}) = \frac{1}{\|\mathbf{c}_o - \mathbf{c}_p\|_2 + \epsilon}$, where ϵ is a small constant to avoid division by zero.

Similarity in Degree Distribution (SD2) SD2 measures structural similarity between two KGs, while addressing SC2D's ineffectiveness when the KGs' entities have tiny local clustering coefficients (e.g., the item KG used by recommender systems is roughly bipartite). In such cases, SC2D always equals roughly zero regardless of perturbation method, thus rendering SC2D useless. Let $\mathbf{d}^r$ denote the $|\mathcal{E}|$-dimensional degree vector for $\mathcal{G}^r$, where the ith element of $\mathbf{d}^r$ is $\deg(e_i)$. Then, the mean degree vectors for $\mathcal{G}$ and $\mathcal{G}'$ are $\mathbf{d}_o = \frac{1}{|\mathcal{R}|}\sum_{r\in\mathcal{R}} \mathbf{d}^r$ and $\mathbf{d}_p = \frac{1}{|\mathcal{R}'|}\sum_{r\in\mathcal{R}'} \mathbf{d}^r$, respectively. Finally, SD2 is defined as $f_{\text{SD2}}(\mathcal{G}, \mathcal{G}^{'}) = \frac{1}{\|\mathbf{d}_o - \mathbf{d}_p\|_2 + \epsilon}$.

4 Methods for Targeted KG Perturbation

We aim to study how a KG's semantics and structure impact NSKG models' downstream performance. To do so, we measure model performance in response to various forms of targeted KG perturbation. While a KG's semantics can be perturbed via its relation types, its structure can be perturbed via its edge connections. Therefore, we design five methods (four heuristic, one RL) for perturbing KG relation types, edge connections, or both.

4.1 Heuristic-Based KG Perturbation

Our four KG perturbation heuristics are as follows: **Relation Swapping (RS)** randomly chooses two edges from $\mathcal{T}$ and swaps their relations. **Relation Replacement (RR)** randomly chooses an edge $(e_1, r_1, e_2) \in \mathcal{T}$, then replaces r_1 with another relation $r_2 = \text{argmin}_{r\in\mathcal{R}}\, s_{\mathcal{G}}(e_1, r, e_2)$. **Edge Rewiring (ER)** randomly chooses an edge $(e_1, r, e_2) \in \mathcal{T}$, then replaces e_2 with another entity $e_3 \in \mathcal{E} \setminus \mathcal{N}_1(e_1)$. **Edge Deletion (ED)** randomly chooses an edge $(e_1, r, e_2) \in \mathcal{T}$ and deletes it. For ED, perturbing all edges means deleting all but 10 edges.

4.2 RL-Based KG Perturbation

We introduce an RL-based approach for perturbing the KG. Given a KG, $\mathcal{G}$, we train a policy to output a perturbed KG, $\mathcal{G}'$, such that ATS, $f_{\text{ATS}}(\mathcal{G}, \mathcal{G}^{'})$, is minimized, while downstream performance, $g(\mathcal{G}^{'})$, is maximized. Specifically, the RL agent is trained to perturb $\mathcal{G}$ via relation replacement, so we call our algorithm **RL-RR**. Because the agent is limited to applying $N = |\mathcal{T}|$ perturbations to $\mathcal{G}$, our RL problem is framed as a finite horizon Markov decision process. In the rest of this section, we define the actions, states, and reward in our RL problem, then explain how RL-RR is implemented. Figure 2 depicts all five proposed perturbation methods.

Actions The action space consists of all possible relation replacements in $\mathcal{G}$, i.e., replacing $(e_1, r, e_2) \in \mathcal{T}$ with (e_1, r', e_2). Since having such a large action space poses computational issues, we decouple each action into a sequence of three *subactions* and operate instead in this smaller subaction space. Hence, a perturbation action at time step t would be $a_t = (a_t^{(0)}, a_t^{(1)}, a_t^{(2)})$. Namely, $a_t^{(0)}$ is sampling entity $e_1 \in \mathcal{E}$; $a_t^{(1)}$ is selecting edge $(e_1, r, e_2) \in \mathcal{T}$; and $a_t^{(2)}$ is selecting relation $r' \in \mathcal{R}$ to replace r in (e_1, r, e_2). To make the policy choose low-ATS perturbations, we further restrict the $a_t^{(2)}$ subaction space to be the K subactions resulting in the lowest ATS. Note that each

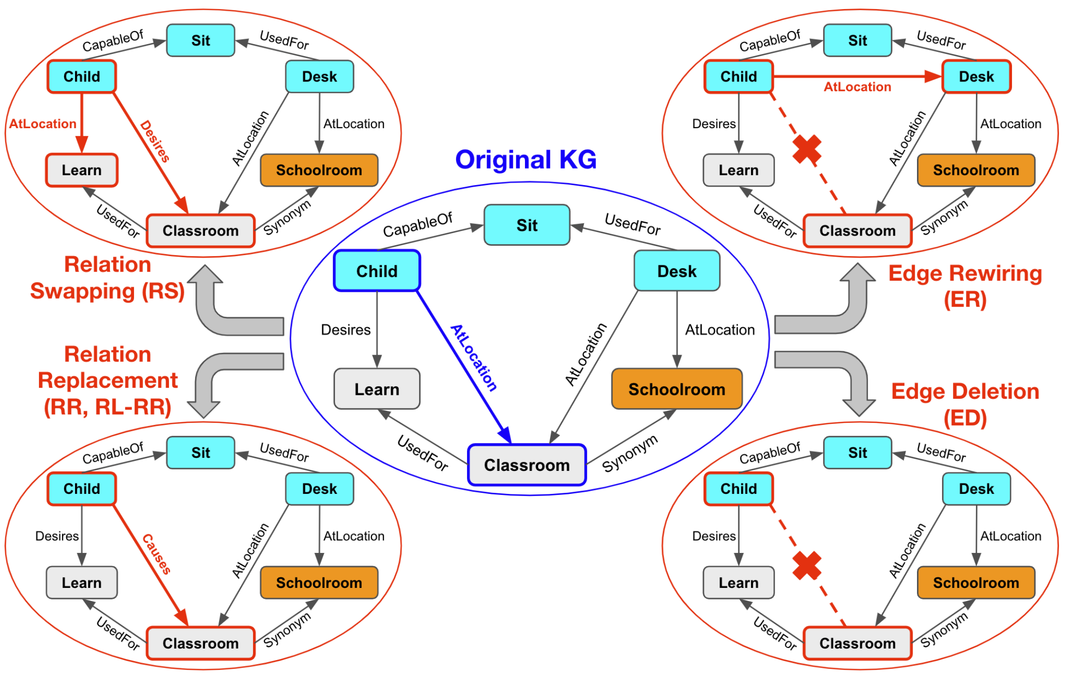

Figure 2: **Proposed KG Perturbation Methods.** We propose four heuristic-based perturbation methods and one RL-based perturbation method. In this diagram, we consider example edge `(Child, AtLocation, Classroom)` within a subgraph of the original ConceptNet KG (shown in blue). We illustrate how this edge (and possibly other edges) changes in response to different perturbation methods (shown in red). Unlike the heuristic-based methods (RS, RR, ER, ED), the RL-based method (RL-RR) is trained to maximize downstream performance and minimize original-perturbed KG semantic similarity.

$a_t^{(i)}$ is represented by its corresponding pre-trained TransE (Bordes et al., 2013) entity, relation, or edge embedding in $\mathcal{G}$. Since these TransE embeddings are not updated by the perturbation policy, we use $a_t^{(i)}$ to refer to both the subaction and subaction embedding. Meanwhile, a_t does not have any representation besides its constituent subaction embeddings.

States The state space is the set of all $\mathcal{G}'$ with the same entities and connectivity structure as $\mathcal{G}$. Here, we make a distinction between state and state embedding. The state at t is the actual KG after t perturbation steps and is denoted as $\mathcal{G}_t$. The state embedding at t is a vector representation of $\mathcal{G}_t$ and is denoted as s_t. To match a_t, we also decouple s_t into *substate* embeddings: $s_t = (s_t^{(0)}, s_t^{(1)}, s_t^{(2)})$.

Reward The reward function pushes the policy to maximize downstream performance. For commonsense QA, higher reward corresponds to lower KL divergence between the predicted and true answer distributions. For item recommendation, we use dev AUC as the reward function.

4.2.1 DQN Architecture and Training

As described above, RL-RR is modeled as an action-subaction hierarchy. At the action (top) level, for t, the policy selects an action a_t given state s_t, then performs a_t on $\mathcal{G}_t$ to obtain $\mathcal{G}_{t+1}$. At the subaction (bottom) level, for index $i \in [0, 1, 2]$ within time step t, the policy selects a subaction $a_t^{(i+1)}$ given $s_t^{(i)}$ and, if any, previous subactions.

At t, the policy takes as input the substate embedding $s_t^{(0)}$. One approach for computing $s_t^{(0)}$ would be to directly encode $\mathcal{G}_t$ with a graph encoder $\mathcal{F}^{\text{graph}}$, such that $s_t^{(0)} = \mathcal{F}^{\text{graph}}(\mathcal{G}_t)$ (Dai et al., 2018; Sun et al., 2020; Ma et al., 2019b). However, since we aim to assess graph encoders' ability to capture KG information, it would not make sense to use a graph encoder for KG perturbation. Instead, we use an LSTM (Hochreiter & Schmidhuber, 1997) to update substate embeddings both within and across time steps, while jointly encoding substate and subaction embeddings. Observe that this means $s_t^{(i)}$ only implicitly captures KG state information via $a_t^{(i-1)}$, since the choice of each subaction is constrained precisely by which entities, relations, or edges are available in $\mathcal{G}_t$.

To train RL-RR, we use the DQN algorithm (Mnih et al., 2015). Abstractly, the goal of DQN is to learn a Q-function $Q(s_t, a_t)$, which outputs the expected reward for taking action a_t in state s_t. In practice, $Q(s_t, a_t)$ is decomposed into a sequential pair of sub-Q-functions: $Q_1(a_t^{(1)} | s_t^{(0)}, a_t^{(0)}) = \langle \text{MLP}(a_t^{(1)}), \text{MLP}(h_t^{(0)}) \rangle$ and $Q_2(a_t^{(2)} | s_t^{(1)}, a_t^{(0)}, a_t^{(1)}) = \langle \text{MLP}(a_t^{(2)}), \text{MLP}(h_t^{(1)}) \rangle$. MLP denotes the vector representation computed by a multi-layer perceptron, while $h_t^{(0)}$ and $h_t^{(1)}$ denote the respective LSTM encodings of $(s_t^{(0)}, a_t^{(0)})$ and $(s_t^{(1)},\ [a_t^{(0)} \oplus a_t^{(1)}])$.

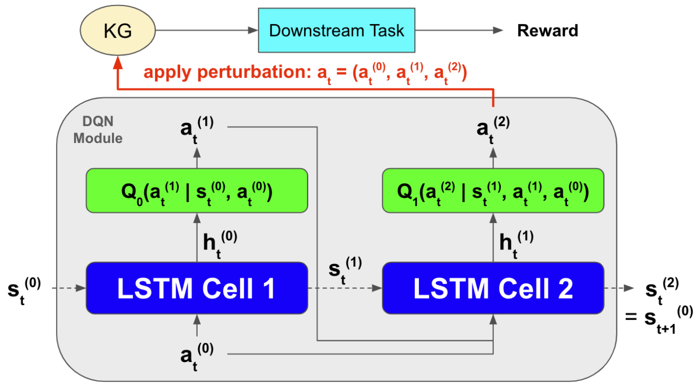
KG
Downstream Task
Reward
apply perturbation: $a_t = (a_t^{(0)}, a_t^{(1)}, a_t^{(2)})$
DQN Module
$a_t^{(1)}$
$a_t^{(2)}$
$Q_0(a_t^{(1)} \mid s_t^{(0)}, a_t^{(0)})$
$Q_1(a_t^{(2)} \mid s_t^{(1)}, a_t^{(1)}, a_t^{(0)})$
$h_t^{(0)}$
$h_t^{(1)}$
$s_t^{(0)}$
LSTM Cell 1
$s_t^{(1)}$
LSTM Cell 2
$s_t^{(2)} = s_{t+1}^{(0)}$
$a_t^{(0)}$

Figure 3: **DQN Architecture for RL-RR**

Figure 3 depicts the perturbation procedure at t. First, we either initialize $s_t^{(0)}$ with a trained embedding weight vector if $t = 0$, or set it to $s_{t-1}^{(2)}$ otherwise. Second, we uniformly sample $a_t^{(0)}$, which is encoded as $h_t^{(0)} = \text{LSTMCell}_1(s_t^{(0)}, a_t^{(0)})$. LSTMCell$_1$ also updates $s_t^{(0)}$ to $s_t^{(1)}$. Third, we compute $Q_1(a_t^{(1)}|s_t^{(0)}, a_t^{(0)})$, which takes $h_t^{(0)}$ as input and outputs $a_t^{(1)}$. Fourth, we encode $a_t^{(1)}$ as $h_t^{(1)} = \text{LSTMCell}_2(s_t^{(1)},\ [a_t^{(0)} \oplus a_t^{(1)}])$. LSTMCell$_2$ also updates $s_t^{(1)}$ to $s_t^{(2)}$. Fifth, we compute $Q_2(a_t^{(2)}|s_t^{(1)}, a_t^{(0)}, a_t^{(1)})$, which takes $h_t^{(1)}$ as input and outputs $a_t^{(2)}$. Note that $a_t^{(1)}$ and $a_t^{(2)}$ are selected ϵ-greedily during training and greedily during evaluation. Finally, using $a_t = (a_t^{(0)}, a_t^{(1)}, a_t^{(2)})$, we perturb $\mathcal{G}_t$ to get $\mathcal{G}_{t+1}$.

Ideally, for each t, we would evaluate $\mathcal{G}_{t+1}$ on the downstream task to obtain the reward. However, downstream evaluation is expensive, so we only compute reward every T time steps. Moreover, for the policy to generalize well, state embeddings $(s_{t-T+1}, \dots, s_{t-1}, s_t)$ should not correlate with the order of actions $(a_{t-T+1}, \dots, a_{t-1}, a_t)$. Thus, for every T time steps during training, we shuffle the last T actions after computing reward, then update the LSTM and sub-Q-functions with respect to the shuffled actions. Doing so encourages state embeddings to be invariant to action order.

5 Experiments

In this section, we test NSKG models on their ability to maintain performance and explainability when the KG has been extensively perturbed. As explained in Section 2 and Figure 1, the model is first trained on a given dataset using the original KG, frozen throughout KG perturbation, then used to compare downstream performance between original KG and perturbed KG. For all models, datasets, and perturbation methods, we measure performance and KG similarity when all $|\mathcal{T}|$ KG edges have been perturbed, averaged over three runs. For a subset of model-dataset-perturbation configurations, we also measure performance as a function of the number of edges perturbed. In addition, we conduct a user study where humans are asked to rate original and perturbed KGs, with respect to readability and usability for solving downstream tasks.

5.1 Commonsense QA

For commonsense QA, the NSKG models we experiment with are RN (with attentional path aggregation) (Lin et al., 2019; Santoro et al., 2017) and MHGRN (Feng et al., 2020), which have been shown to outperform non-KG models (Devlin et al., 2018; Liu et al., 2019) and a number of NSKG models (Lin et al., 2019; Ma et al., 2019a; Wang et al., 2019c; Schlichtkrull et al., 2018) on this task. For both models, we use a BERT-Base (Devlin et al., 2018) text encoder. We evaluate on the CommonsenseQA (CSQA) (Talmor et al., 2018) and OpenBookQA (OBQA) (Mihaylov et al., 2018) datasets, using ConceptNet (Speer et al., 2016) as the KG. Performance is measured using accuracy, which is the standard metric for commonsense QA (Lin et al., 2019; Feng et al., 2020).

CSQA Results for CSQA are given in Table 1. For RN and MHGRN, we see that RL-RR achieves slightly worse accuracy than Original KG, while RS, RR, and ER perform on par with No KG. For both models, ED performs noticeably worse than No KG. We also observe that perturbed KGs produced by RS and ED have high ATS (i.e., semantic similarity to original KG), while RR, ER, and RL-RR achieve relatively low ATS.

OBQA Results for OBQA are shown in Table 2. For RN, we see that RL-RR actually obtains better accuracy than Original KG. For MHGRN, RL-RR yields marginally worse accuracy than Original

Table 1: **Comparison of Perturbation Methods on CSQA.** We follow the standard protocol of reporting CSQA test accuracy on the in-house data split from Lin et al. (2019), as official test labels are not available.

	CSQA							
	RN				**MHGRN**			
Method	Acc (↑)	ATS (↓)	SC2D (↓)	SD2 (↓)	Acc (↑)	ATS (↓)	SC2D (↓)	SD2 (↓)
No KG	53.41	-	-	-	53.41	-	-	-
Original KG	56.87	0.940	-	-	57.21	0.940	-	-
Relation Swapping (RS)	53.42	0.831	0.168	6.20E-3	53.42	0.831	0.168	6.20E-3
Relation Replacement (RR)	53.42	0.329	**0.100**	1.70E-3	52.22	0.329	**0.100**	**1.70E-3**
Edge Rewiring (ER)	53.42	0.505	0.131	2.31E-3	52.22	0.505	0.131	2.31E-3
Edge Deletion (ED)	52.21	0.933	0.144	2.00E-3	51.00	0.933	0.144	2.00E-3
RL-RR	**55.21**	**0.322**	0.102	**1.66E-3**	**55.52**	**0.314**	0.101	1.78E-3

Table 2: **Comparison of Perturbation Methods on OBQA**

	OBQA							
	RN				**MHGRN**			
Method	Acc (↑)	ATS (↓)	SC2D (↓)	SD2 (↓)	Acc (↑)	ATS (↓)	SC2D (↓)	SD2 (↓)
No KG	62.00	-	-	-	62.00	-	-	-
Original KG	66.80	0.934	-	-	68.00	0.934	-	-
Relation Swapping (RS)	67.00	0.857	0.189	7.79E-3	67.30	0.857	0.189	7.79E-3
Relation Replacement (RR)	66.80	0.269	0.105	1.84E-3	67.60	0.269	0.105	1.84E-3
Edge Rewiring (ER)	66.60	0.620	0.172	7.31E-3	67.00	0.620	0.172	7.31E-3
Edge Deletion (ED)	66.80	0.923	0.155	2.19E-3	67.60	0.923	0.155	2.19E-3
RL-RR	**67.30**	**0.255**	**0.108**	**1.79E-4**	**67.70**	**0.248**	**0.104**	**1.75E-4**

KG. Meanwhile, for both RN and MHGRN, all heuristics uniformly achieve similar accuracy as Original KG, which itself significantly outperforms No KG.

Analysis Tables 1-2 demonstrate that perturbing a KG does not necessarily imply decreased performance, nor does it guarantee the creation of invalid or novel facts. As shown by the KG similarity scores, some perturbation methods cause greater semantic or structural KG changes than others. While ATS varies considerably across perturbation methods, SC2D and SD2 are quite low for all perturbation methods, indicating consistently low structural similarity between original and perturbed KG. RL-RR and RR collectively have the lowest SC2D and SD2 for CSQA, while RL-RR has the lowest SC2D and SD2 for OBQA. Notably, across all perturbation methods and models, RL-RR attains the highest accuracy while also having the lowest KG similarity scores overall. The results of a T-test (three runs for both models) show that RL-RR achieves a statistically significant improvement over its heuristic counterpart, RR. Still, even RR has a fairly high accuracy to KG similarity ratio. This suggests that our NSKG models are not using the KG in a faithful way, since RL-RR and RR can both achieve high performance despite extensively corrupting the original KG's semantic and structural information.

5.2 Item Recommendation

The NSKG recommender systems we consider are KGCN (Wang et al., 2019b) and RippleNet (Wang et al., 2018b). We evaluate these models on the Last.FM (Rendle, 2012) and MovieLens-20M (Harper & Konstan, 2016) datasets, using the item KG from (Wang et al., 2019a). As mentioned in Section 1, item KGs have been shown to benefit recommender systems in cold start scenarios (Wang et al., 2018b). Therefore, following Wang et al. (2018b), we simulate a cold start scenario by using only 20% and 40% of the train set for Last.FM and Movie Lens-20M, respectively. Performance is measured using AUC, which is the standard metric for item recommendation (Wang et al., 2019b; 2018b). Since the item KG is almost bipartite, SC2D is not meaningful here, since the local clustering coefficient of each item in the KG is extremely small (Section 3). Thus, for item recommendation, we do not report SC2D.

Last.FM Results for Last.FM are displayed in Table 3. For both KGCN and RippleNet, we see that RS, RR, and RL-RR achieve about the same AUC as Original KG, with RL-RR slightly outperforming Original KG. Furthermore, ER performs similarly to Original KG for KGCN, but considerably worse for RippleNet. ED's AUC is on par with No KG's for KGCN and much lower than No KG's for RippleNet. We also observe that the perturbed KGs produced by ED have high ATS, while RS, RR, ER, and RL-RR achieve more modest ATS scores.

Table 3: **Comparison of Perturbation Methods on Last.FM**

	Last.FM					
	KGCN			Ripplenet		
Method	Acc (↑)	ATS (↓)	SD2 (↓)	Acc (↑)	ATS (↓)	SD2 (↓)
No KG	50.75	-	-	50.75	-	-
Original KG	55.99	0.972	-	56.23	0.972	-
Relation Swapping (RS)	55.98	0.681	3.05E-2	56.23	0.681	3.05E-2
Relation Replacement (RR)	55.98	0.415	0.339	56.22	0.415	0.339
Edge Rewiring (ER)	55.98	0.437	1.89E-2	53.74	0.437	1.89E-2
Edge Deletion (ED)	50.96	0.941	3.38E-3	45.98	0.941	0.3.38E-3
RL-RR	**56.04**	**0.320**	**1.30E-3**	**56.28**	**0.310**	**1.20E-3**

Table 4: **Comparison of Perturbation Methods on MovieLens-20M**

	Last.FM					
	KGCN			Ripplenet		
Method	Acc (↑)	ATS (↓)	SD2 (↓)	Acc (↑)	ATS (↓)	SD2 (↓)
No KG	91.30	-	-	91.30	-	-
Original KG	96.62	0.960	-	97.46	0.960	-
Relation Swapping (RS)	**96.62**	0.678	6.14E-4	97.46	0.678	6.14E-4
Relation Replacement (RR)	96.50	0.413	**7.74E-5**	97.45	0.413	**7.74E-5**
Edge Rewiring (ER)	96.24	0.679	4.44E-4	93.42	0.679	4.44E-4
Edge Deletion (ED)	90.36	0.982	1.02E-4	90.22	0.982	0.1.02E-4
RL-RR	96.53	**0.401**	2.23E-4	97.25	**0.268**	2.21E-4

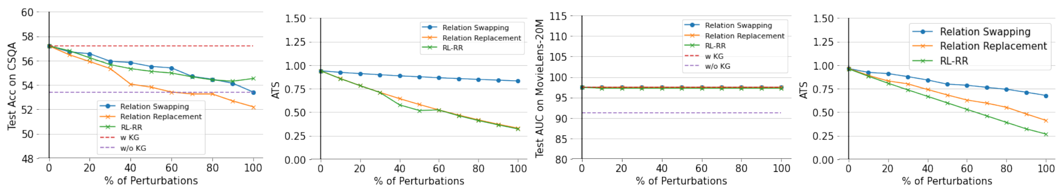

(a) CSQA Acc (b) CSQA ATS (c) MovieLens-20M AUC (d) MovieLens-20M ATS

Figure 4: **Varying Perturbation Level.** Performance and ATS with respect to perturbation level, for MHGRN on CSQA and RippleNet on MovieLens-20M. Horizontal axis denotes percentage of perturbed KG edges.

MovieLens-20M Results for MovieLens-20M are displayed in Table 4. For both KGCN and RippleNet, we find that relation-based perturbation methods tend to perform on par with Original KG. Here, ER is the better of the two edge-based perturbation methods, performing about the same as Original KG for KGCN, but noticeably worse for RippleNet. Somehow, for both KGCN and RippleNet, ED achieves even worse AUC than No KG. On the other hand, we see that ED achieves very high ATS, while RS, RR, ER, and RL-RR achieve more modest ATS scores.

Analysis Like in commonsense QA, Tables 3-4 show that NSKG models can perform well even when the KG has been drastically perturbed. Using the T-test with three runs, for almost all perturbation methods, we find a statistically insignificant difference between the perturbed KG's AUC and the original KG's AUC. Whereas ATS again varies greatly across perturbation methods, all perturbation methods have fairly low SD2 (except RR on Last.FM), indicating that structural similarity between original and perturbed KG is consistently low. In particular, across both datasets and models, RL-RR has the highest AUC overall, while also having the lowest KG similarity scores overall. This serves as additional evidence that the model is not using the KG faithfully, since RL-RR achieves high performance despite significantly perturbing the original KG's semantic and structural information.

5.3 Auxiliary Experiments and Analysis

Varying Perturbation Level For a subset of model-dataset-perturbation settings, we measure the performance and ATS of various perturbation methods as a function of the percentage of KG edges perturbed. For MHGRN on CSQA, Figure 4a shows that, across all levels of perturbation, RL-RR maintains higher accuracy than No KG. Meanwhile, RS's accuracy reaches No KG's accuracy at 100% perturbation, and RR's does so at 60% perturbation. In Figure 4b, we see that RL-RR's and RR's ATS drop significantly as the perturbation percentage increases, whereas RS's ATS remains quite high even at 100% perturbation. For RippleNet on MovieLens-20M, Figure 4c shows a flat

Method	CSQA		OBQA	
	RN	MHGRN	RN	MHGRN
No KG	53.41	53.41	62.00	62.00
Orignal KG	56.87	57.21	66.80	68.00
Zero Subgraph Emb.	53.10	53.99	64.80	66.40
Rand. Subgraph Emb.	52.60	52.48	64.75	65.90
Rand. Ent./Rel. Emb.	53.02	54.03	64.45	64.85

Table 5: **Noisy Baselines for Commonsense QA.** Noisy baseline accuracy on CSQA and OBQA.

Method	Last.FM		MovieLens-20M	
	KGCN	RippleNet	KGCN	RippleNet
No KG	50.75	50.75	91.30	91.30
Original KG	55.99	56.23	96.62	97.46
Rand. Ngbd.	55.91	51.04	96.21	92.11

Table 6: **Noisy Baselines for Item Recommendation.** Noisy baseline AUC on Last.FM and MovieLens-20M.

performance curve for all perturbation methods. Meanwhile, for all perturbation methods in Figure 4d, ATS decreases steadily as the number of perturbations increases, with RL-RR's ATS dropping most. These findings support the hypothesis that KG perturbation does not imply performance decrease or KG corruption. Building on the results of previous experiments, in both model-dataset settings, RL-RR largely maintains the model's performance despite also heavily perturbing the KG's semantics. Interestingly, for RippleNet on MovieLens-20M, performance is completely unaffected by KG perturbation, even though the KG's semantic information is apparently being corrupted.

Noisy Baselines To see if KGs produced by our perturbation methods are capturing more than just random noise, we compare them to several noisy baselines. Table 5 contains results for three noisy baselines on commonsense QA: (1) replace subgraph embedding with zero vector, (2) replace subgraph embedding with random vector, and (3) replace entity/relation embeddings with random vectors. For CSQA, the noisy baselines perform noticeably worse than both Original KG and RL-RR, while being on par with No KG (Table 1). For OBQA, the noisy baselines' performance is slightly better than No KG, but considerably worse than not only Original KG, but all of the perturbation methods (Table 2). Table 6 displays results for our noisy baseline in item recommendation, which entails randomizing each entity's neighborhood. We find that KGCN performs about the same for this noisy baseline as for Original KG and our best perturbation methods, whereas RippleNet performs much worse (Tables 3-4). RippleNet may be more sensitive than KGCN to entity neighbor randomization because RippleNet considers directed edges. This is supported by RippleNet's performance dropping when we perturb edge connections (Tables 3-4). In both tasks, the noisy baselines show that our perturbation methods yield KGs that capture measurably useful information beyond just noise. For KGCN, the unexpected discovery that noisy baselines perform similarly to Original KG suggest that even noisy KGs can contain useful information for NSKG models.

Human Evaluation of KG Explanations We conduct a user study to measure KGs' ability to provide plausible explanations. Here, we consider the original KG and the RL-RR KG. For both KGs, we sample 30 questions from the CSQA and OBQA test sets which were correctly answered by MHGRN. For each question, we retrieve the top-scoring path for each answer choice via MHGRN's path decoder attention. We then ask three human annotators to rate each path for readability and usability, with ratings aggregated via majority voting. Readability ($[0, 1]$ scale) is whether the path makes sense. Usability ($[0, 1, 2]$ scale) is whether the path is relevant to the given question-answer pair. We obtain a Fleiss' κ of 0.1891, indicating slight inter-annotator agreement. To illustrate, we provide examples of explanation paths and their consensus ratings. Given the question *James chose to not to print the cards, because he wanted to be more personal. What type of cards did he choose, instead?*, the Original KG path is PRINT —[ANTONYM]→ HANDWRITTEN (Read=1.0; Use=2.0), and the RL-RR path is PRINT — [NOTDESIRES]→ HANDWRITTEN (Read=0.0; Use=0.0). Here, the Original KG path seems plausible, but the RL-RR path does not.

Method	CSQA		OBQA	
	Read	Use	Read	Use
Orig. KG	0.081	0.720	0.111	0.714
RL-RR	0.115	0.706	0.111	0.397

Table 7: **Human Evaluation of KG Explanations.** Human ratings for readability (Read) and usability (Use) of KG paths.

In Table 7, we see that Original KG and RL-RR scored very similarly, except for RL-RR being much worse on OBQA. This shows that RL-RR can maintain model performance while corrupting the KG semantically and structurally. Nonetheless, Original KG and RL-RR both got relatively low ratings overall, indicating the implausibility of NSKG models' explanations. OBQA's much larger usability gap between Original KG and RL-RR can be explained by the fact that CSQA is constructed from ConceptNet. Every CSQA question-answer is based on ConceptNet entities/relations, so a random ConceptNet subgraph is more likely to have semantic overlap with a CSQA question-answer than with an OBQA question-answer. Hence, a perturbed ConceptNet subgraph may also be more likely to overlap with a CSQA question-answer, and so perturbing the KG might have a smaller impact on human judgments of CSQA path usability. This does not say anything about the model's performance on CSQA and OBQA, as high model performance does not necessarily imply high explanation quality. In fact, our user study disproves this connection.

Validation of KG Similarity Metrics Using the results of our human evaluation, we validate our three proposed KG similarity metrics: ATS, SC2D and SD2. We find that the Pearson correlation coefficient between the human evaluation scores in Table 7 and the three KG similarity scores in Tables 1-2 are 0.845, 0.932 and 0.932, respectively. This indicates high correlation and demonstrates that the KG similarity metrics aptly capture how well a perturbed KG preserves semantic and structural information from its original KG.

Why do perturbed KGs sometimes perform better than the original KG? In our experiments, relation-based perturbations (RS, RR, RL-RR) generally outperform edge-based perturbations (ER, ED). Also, we have found that the original KG can contain noisy relation annotations which are sometimes "corrected" by relation-based perturbations. In certain cases, this may result in the perturbed KG achieving slightly higher performance than the original KG (RR and RL-RR for RN-CSQA; RL-RR for Last.FM). Similarly, in our user study, despite all questions being correctly answered by the model, there were some RL-RR explanations that received higher readability/usability ratings than their original KG counterparts. Although the original KG achieved higher human ratings than the RL-RR KG did overall, both KGs still achieved relatively low ratings with respect to our scales. While our main argument centers on NSKG models' flaws, this counterintuitive finding suggests that KGs themselves are flawed too, but in a way that can be systematically corrected.

6 Related Work

KG-Augmented Models For various downstream tasks, KGs are commonly used to improve performance by augmenting machine learning models with external knowledge. In fact, the successes of pretrained language models (LMs) in natural language processing (NLP) have been hypothesized to stem from such LMs' ability to probe a latent knowledge base (Petroni et al., 2019). In the past, KGs have been used in various tasks such as commonsense QA (Lin et al., 2019; Shen et al., 2020; Lv et al., 2020; Musa et al., 2019), recommender systems (Wang et al., 2019b; 2020; Song et al., 2019; Cao et al., 2019), NLI, (Wang et al., 2019c) and many others (Chen et al., 2019; Kapanipathi et al.), greatly boosting KG-augmented model performance compared to non-KG methods. KGs have also been regarded as an important way to make the model more interpretable and generate explanations (Lin et al., 2019; Zhang et al., 2019; Song et al., 2019; Cao et al., 2019; Gao et al., 2019; Ai et al., 2018).

Adversarial Perturbation of Graphs Inspired by adversarial learning in computer vision and NLP, there have been many recent works investigating adversarial perturbations in the graph learning framework (Chen et al., 2020). Like our work, these works also involve perturbing a graph, although their purpose for doing so is different. Whereas existing works primarily aim to adversarially perturb the graph minimally while having maximum impact on performance, our goal is to use graph perturbations to analyze the faithfulness of NSKG models in using KG information. A variety of paradigms have been proposed for perturb the graph, including gradient-based methods (Chen et al., 2018; Bojchevski & Günnemann, 2019; Wu et al., 2019), RL-based methods (Ma et al., 2019b; Dai et al., 2018), and autoencoder-based methods (Chen et al., 2018). Moreover, few existing works on graph perturbations have considered heterogeneous graphs like KGs. Ma et al. (2019b) use an RL-based adversarial perturbation policy, but they only consider homogeneous graphs in their framework. Meanwhile, our work considers a KG, which is naturally heterogeneous. To the best of our knowledge, this is the first work to use graph perturbations for analyzing the faithfulness of NSKG models in using KG information and providing explanations.

7 Conclusion

In this paper, we analyze the effects of strategically perturbed KGs on NSKG model predictions. Using four heuristics and a RL policy, we show that KGs can be perturbed in way that drastically changes their semantics and structure, while still preserving the model's downstream performance. Furthermore, we conduct a user study to demonstrate that both perturbed and unperturbed KGs struggle to facilitate plausible explanations of the model's predictions. Note that our proposed KG perturbation methods merely serve as analytical tools and are not intended to directly improve performance or explanation quality. Still, we believe our findings can guide future work on designing NSKG models that are better in these aspects. Additionally, our results suggest that NSKG models can be robust to noisy KG data. Even when the KG contains a fairly small amount of signal, these models are somehow able to leverage it. This could be a useful property in situations where it is not practical to obtain fully clean KG annotations.

REFERENCES

Qingyao Ai, Vahid Azizi, Xu Chen, and Yongfeng Zhang. Learning heterogeneous knowledge base embeddings for explainable recommendation. *Algorithms*, 11(9):137, 2018.

Aleksandar Bojchevski and Stephan Günnemann. Adversarial attacks on node embeddings via graph poisoning. In *International Conference on Machine Learning*, pp. 695–704. PMLR, 2019.

Antoine Bordes, Nicolas Usunier, Alberto Garcia-Duran, Jason Weston, and Oksana Yakhnenko. Translating embeddings for modeling multi-relational data. In *Advances in neural information processing systems*, pp. 2787–2795, 2013.

Yixin Cao, Xiang Wang, Xiangnan He, Zikun Hu, and Tat-Seng Chua. Unifying knowledge graph learning and recommendation: Towards a better understanding of user preferences. In *The world wide web conference*, pp. 151–161, 2019.

Daoyuan Chen, Yaliang Li, Min Yang, Hai-Tao Zheng, and Ying Shen. Knowledge-aware textual entailment with graph attention network. *Proceedings of the 28th ACM International Conference on Information and Knowledge Management*, 2019.

Jinyin Chen, Yangyang Wu, Xuanheng Xu, Yixian Chen, Haibin Zheng, and Qi Xuan. Fast gradient attack on network embedding. *arXiv preprint arXiv:1809.02797*, 2018.

Liang Chen, Jintang Li, Jiaying Peng, Tao Xie, Zengxu Cao, Kun Xu, Xiangnan He, and Zibin Zheng. A survey of adversarial learning on graphs. *arXiv preprint arXiv:2003.05730*, 2020.

Hanjun Dai, Hui Li, Tian Tian, Xin Huang, Lin Wang, Jun Zhu, and Le Song. Adversarial attack on graph structured data. *arXiv preprint arXiv:1806.02371*, 2018.

Jacob Devlin, Ming-Wei Chang, Kenton Lee, and Kristina Toutanova. Bert: Pre-training of deep bidirectional transformers for language understanding. *arXiv preprint arXiv:1810.04805*, 2018.

Giorgio Fagiolo. Clustering in complex directed networks. *Physical Review E*, 76(2):026107, 2007.

Yanlin Feng, Xinyue Chen, Bill Yuchen Lin, Peifeng Wang, Jun Yan, and Xiang Ren. Scalable multi-hop relational reasoning for knowledge-aware question answering. *arXiv preprint arXiv:2005.00646*, 2020.

Jingyue Gao, Xiting Wang, Yasha Wang, and Xing Xie. Explainable recommendation through attentive multi-view learning. In *Proceedings of the AAAI Conference on Artificial Intelligence*, volume 33, pp. 3622–3629, 2019.

F. Maxwell Harper and Joseph A. Konstan. The movielens datasets: History and context. *ACM Trans. Interact. Intell. Syst.*, 5(4):19:1–19:19, 2016.

Sepp Hochreiter and Jürgen Schmidhuber. Long short-term memory. *Neural computation*, 9(8): 1735–1780, 1997.

Pavan Kapanipathi, Veronika Thost, Siva Sankalp Patel, Spencer Whitehead, Ibrahim Abdelaziz, Avinash Balakrishnan, Maria Chang, Kshitij P Fadnis, R Chulaka Gunasekara, Bassem Makni, et al. Infusing knowledge into the textual entailment task using graph convolutional networks.

Xiang Li, Aynaz Taheri, Lifu Tu, and Kevin Gimpel. Commonsense knowledge base completion. In *Proceedings of the 54th Annual Meeting of the Association for Computational Linguistics (Volume 1: Long Papers)*, pp. 1445–1455, Berlin, Germany, August 2016. Association for Computational Linguistics. doi: 10.18653/v1/P16-1137. URL `https://www.aclweb.org/anthology/P16-1137`.

Bill Yuchen Lin, Xinyue Chen, Jamin Chen, and Xiang Ren. Kagnet: Knowledge-aware graph networks for commonsense reasoning. In *Proceedings of the 2019 Conference on Empirical Methods in Natural Language Processing and the 9th International Joint Conference on Natural Language Processing (EMNLP-IJCNLP)*, pp. 2822–2832, 2019.

Yinhan Liu, Myle Ott, Naman Goyal, Jingfei Du, Mandar Joshi, Danqi Chen, Omer Levy, Mike Lewis, Luke Zettlemoyer, and Veselin Stoyanov. Roberta: A robustly optimized bert pretraining approach. *arXiv preprint arXiv:1907.11692*, 2019.

Shangwen Lv, Daya Guo, Jingjing Xu, Duyu Tang, Nan Duan, Ming Gong, Linjun Shou, Daxin Jiang, Guihong Cao, and Songlin Hu. Graph-based reasoning over heterogeneous external knowledge for commonsense question answering. In *AAAI*, 2020.

Kaixin Ma, Jonathan Francis, Quanyang Lu, Eric Nyberg, and Alessandro Oltramari. Towards generalizable neuro-symbolic systems for commonsense question answering. *arXiv preprint arXiv:1910.14087*, 2019a.

Yao Ma, Suhang Wang, Tyler Derr, Lingfei Wu, and Jiliang Tang. Attacking graph convolutional networks via rewiring. *arXiv preprint arXiv:1906.03750*, 2019b.

Todor Mihaylov, Peter Clark, Tushar Khot, and Ashish Sabharwal. Can a suit of armor conduct electricity? a new dataset for open book question answering. In *Proceedings of the 2018 Conference on Empirical Methods in Natural Language Processing*, pp. 2381–2391, Brussels, Belgium, October-November 2018. Association for Computational Linguistics. doi: 10.18653/v1/D18-1260. URL `https://www.aclweb.org/anthology/D18-1260`.

Volodymyr Mnih, Koray Kavukcuoglu, David Silver, Andrei A Rusu, Joel Veness, Marc G Bellemare, Alex Graves, Martin Riedmiller, Andreas K Fidjeland, Georg Ostrovski, et al. Human-level control through deep reinforcement learning. *nature*, 518(7540):529–533, 2015.

Ryan Musa, Xiaoyan Wang, Achille Fokoue, Nicholas Mattei, Maria Chang, Pavan Kapanipathi, Bassem Makni, Kartik Talamadupula, and Michael Witbrock. Answering science exam questions using query reformulation with background knowledge. In *Automated Knowledge Base Construction (AKBC)*, 2019. URL `https://openreview.net/forum?id=HJxYZ-5paX`.

Jukka-Pekka Onnela, Jari Saramäki, János Kertész, and Kimmo Kaski. Intensity and coherence of motifs in weighted complex networks. *Physical Review E*, 71(6):065103, 2005.

Fabio Petroni, Tim Rocktäschel, Patrick Lewis, Anton Bakhtin, Yuxiang Wu, Alexander H Miller, and Sebastian Riedel. Language models as knowledge bases? *arXiv preprint arXiv:1909.01066*, 2019.

Steffen Rendle. Factorization machines with libfm. *ACM Transactions on Intelligent Systems and Technology*, 3(3):57:1–57:22, 2012.

Adam Santoro, David Raposo, David G Barrett, Mateusz Malinowski, Razvan Pascanu, Peter Battaglia, and Timothy Lillicrap. A simple neural network module for relational reasoning. In *Advances in neural information processing systems*, pp. 4967–4976, 2017.

Jari Saramäki, Mikko Kivelä, Jukka-Pekka Onnela, Kimmo Kaski, and Janos Kertesz. Generalizations of the clustering coefficient to weighted complex networks. *Physical Review E*, 75(2): 027105, 2007.

Michael Schlichtkrull, Thomas N Kipf, Peter Bloem, Rianne Van Den Berg, Ivan Titov, and Max Welling. Modeling relational data with graph convolutional networks. In *European Semantic Web Conference*, pp. 593–607. Springer, 2018.

Tao Shen, Yi Mao, Pengcheng He, Guodong Long, Adam Trischler, and Weizhu Chen. Exploiting structured knowledge in text via graph-guided representation learning. *ArXiv*, abs/2004.14224, 2020.

Weiping Song, Zhijian Duan, Ziqing Yang, Hao Zhu, Ming Zhang, and Jian Tang. Explainable knowledge graph-based recommendation via deep reinforcement learning. *ArXiv*, abs/1906.09506, 2019.

Robyn Speer, Joshua Chin, and Catherine Havasi. Conceptnet 5.5: An open multilingual graph of general knowledge. *arXiv preprint arXiv:1612.03975*, 2016.

Yiwei Sun, Suhang Wang, Xianfeng Tang, Tsung-Yu Hsieh, and Vasant Honavar. Adversarial attacks on graph neural networks via node injections: A hierarchical reinforcement learning approach. In *Proceedings of The Web Conference 2020*, pp. 673–683, 2020.

Alon Talmor, Jonathan Herzig, Nicholas Lourie, and Jonathan Berant. Commonsenseqa: A question answering challenge targeting commonsense knowledge. *arXiv preprint arXiv:1811.00937*, 2018.

Hongwei Wang, Fuzheng Zhang, Min Hou, Xing Xie, Minyi Guo, and Qi Liu. Shine: Signed heterogeneous information network embedding for sentiment link prediction. In *Proceedings of the Eleventh ACM International Conference on Web Search and Data Mining*, pp. 592–600, 2018a.

Hongwei Wang, Fuzheng Zhang, Jialin Wang, Miao Zhao, Wenjie Li, Xing Xie, and Minyi Guo. Ripplenet: Propagating user preferences on the knowledge graph for recommender systems. In *Proceedings of the 27th ACM International Conference on Information and Knowledge Management*, pp. 417–426, 2018b.

Hongwei Wang, Fuzheng Zhang, Mengdi Zhang, Jure Leskovec, Miao Zhao, Wenjie Li, and Zhongyuan Wang. Knowledge-aware graph neural networks with label smoothness regularization for recommender systems. In *Proceedings of the 25th ACM SIGKDD International Conference on Knowledge Discovery & Data Mining*, pp. 968–977, 2019a.

Hongwei Wang, Miao Zhao, Xing Xie, Wenjie Li, and Minyi Guo. Knowledge graph convolutional networks for recommender systems. In *The world wide web conference*, pp. 3307–3313, 2019b.

Xiang Wang, Yao-Kun Xu, Xiangnan He, Yixin Cao, Meng Wang, and Tat-Seng Chua. Reinforced negative sampling over knowledge graph for recommendation. *Proceedings of The Web Conference 2020*, 2020.

Xiaoyan Wang, Pavan Kapanipathi, Ryan Musa, Mo Yu, Kartik Talamadupula, Ibrahim Abdelaziz, Maria Chang, Achille Fokoue, Bassem Makni, Nicholas Mattei, et al. Improving natural language inference using external knowledge in the science questions domain. In *Proceedings of the AAAI Conference on Artificial Intelligence*, volume 33, pp. 7208–7215, 2019c.

Huijun Wu, Chen Wang, Yuriy Tyshetskiy, Andrew Docherty, Kai Lu, and Liming Zhu. Adversarial examples on graph data: Deep insights into attack and defense. *arXiv preprint arXiv:1903.01610*, 2019.

Bishan Yang, Wen tau Yih, Xiaodong He, Jianfeng Gao, and Li Deng. Embedding entities and relations for learning and inference in knowledge bases, 2015.

Wen Zhang, Bibek Paudel, Wei Zhang, Abraham Bernstein, and Huajun Chen. Interaction embeddings for prediction and explanation in knowledge graphs. *Proceedings of the Twelfth ACM International Conference on Web Search and Data Mining*, 2019.